Atg7-dependent canonical autophagy regulates the degradation of aquaporin 2 in prolonged hypokalemia

Wan-Young Kim[1], Sun Ah Nam[1], Arum Choi[1], Yu-Mi Kim[1], Sang Hee Park[2], Hong Lim Kim[3], Hyang Kim[4], Ki-Hwan Han[5], Chul Woo Yang[6], Myung-Shik Lee[7], Yong Kyun Kim[1,6] & Jin Kim[1]

[1]Department of Anatomy and Cell Death Disease Research Center, College of Medicine, The Catholic University of Korea, Seoul, Korea. [2]Institute of Clinical Medicine Research of Bucheon St. Mary's Hospital, Bucheon, Korea. [3]Integrative Research Support Center, College of Medicine, The Catholic University of Korea, Seoul, Korea. [4]Division of Nephrology, Kangbuk Samsung Hospital, Sungkyunkwan University, School of Medicine, Seoul, Korea. [5]Department of Anatomy, Ewha Womans University School of Medicine, Seoul, Korea. [6]Department of Internal Medicine, College of Medicine, The Catholic University of Korea, Seoul, Korea. [7]Severance Biomedical Science Institute, College of Medicine, Yonsei University, Seoul, Korea.

Correspondence: Jin Kim, M.D., Ph.D.

Address: Department of Anatomy and Cell Death Disease Research Center, College of Medicine, The Catholic University of Korea, Seoul, Korea, 222 Banpo-Daero, Seocho-Ku, Seoul, 06591, Korea

Telephone: 82-2-2258-7258

Fax: 82-2-536-3110

E mail: jinkim@catholic.ac.kr

Correspondence: Yong Kyun Kim, M.D., Ph.D.

Address: Department of Internal Medicine, Bucheon St. Mary's Hospital, College of Medicine, The Catholic University of Korea, 327 Sosa-ro, Bucheon, Gyeonggi-do, 14647 Korea

Telephone: 82-32-340-7019

Fax: 82-32-340-2667

E mail: drkimyk@catholic.ac.kr

Supplementary Information

Supplementary Table S1. Effect of AQP2-specific deficiency of Atg7 on kidney weight and biochemical parameters.

		Atg7$^{f/f}$		*Atg7*$^{\Delta PC}$	
		Control	K^+-depleted	Control	K^+-depleted
Weight	Body weight (g)	22.5 ± 0.5	19.5 ± 1.26**	24.5 ± 1.63**	23.3 ± 1.31^{+}
	Kidney weight (g)	0.16 ± 0.01	0.15 ± 0.02	0.17 ± 0.02	0.19 ± 0.02$^{**/++}$
	KW/BW (%)	100 ± 8.43	115.15 ± 10.10*	108.65 ± 1.38	123.88 ± 8.05$^{*/\#}$
Blood	Plasma Na^+ (mmol/L)	150.2 ± 1.8	147.4 ± 2.1	150.2 ± 2.0	153.2 ± 2.1$^{*/+/\#}$
	Plasma K^+ (mmol/L)	3.89 ± 0.32	2.97± 0.26**	4.27 ± 0.30	2.28 ± 0.25$^{**/++/\#\#}$
	Plasma Cl^- (mmol/L)	112.8 ± 2.4	113.3 ± 1.5	114.2 ± 3.8	119.5 ± 4.1$^{*/+/\#}$
	BUN (mg/dL)	27.2 ± 5.9	30.8 ± 4.49	27.0 ± 2.65	47.00 ± 7.79$^{*/+/\#}$
Urine	Urine volume (ml)	0.56 ± 0.37	2.48 ± 1.36**	2.37 ± 0.67**	3.02 ± 0.81$^{**/+/\#}$
	Osmolality (mosmol/kgH_2O)	2244.1 ± 421	1168.1 ± 418**	1525.7 ± 401**	974 ± 185$^{**/+/\#\#}$
	Urine Na^+ (mmol/L)	70.7 ± 18.0	38.1 ± 16.8*	52.1 ± 20.0*	26.9 ± 6.2$^{*/+/\#}$
	Urine K^+ (mmol/L)	137.6 ± 16.3	13.7 ± 6.0**	105.2 ± 32.2**	15.3 ± 3.7$^{**/\#\#}$
	Urine Cl^- (mmol/L)	132.1 ± 31.1	61.3 ± 24.9*	95.9 ± 33.2*	67.9 ± 18.0$^{*/+/\#}$

t-test vs. *Atg7*$^{f/f}$ Control * $P < 0.05$, ** $P < 0.001$

t-test vs. *Atg7*$^{f/f}$ K^+-depleted + $P < 0.05$, ++ $P < 0.001$

t-test vs. *Atg7*$^{\Delta PC}$ Control # $P < 0.05$, ## $P < 0.001$

All values are the means ± SEM.

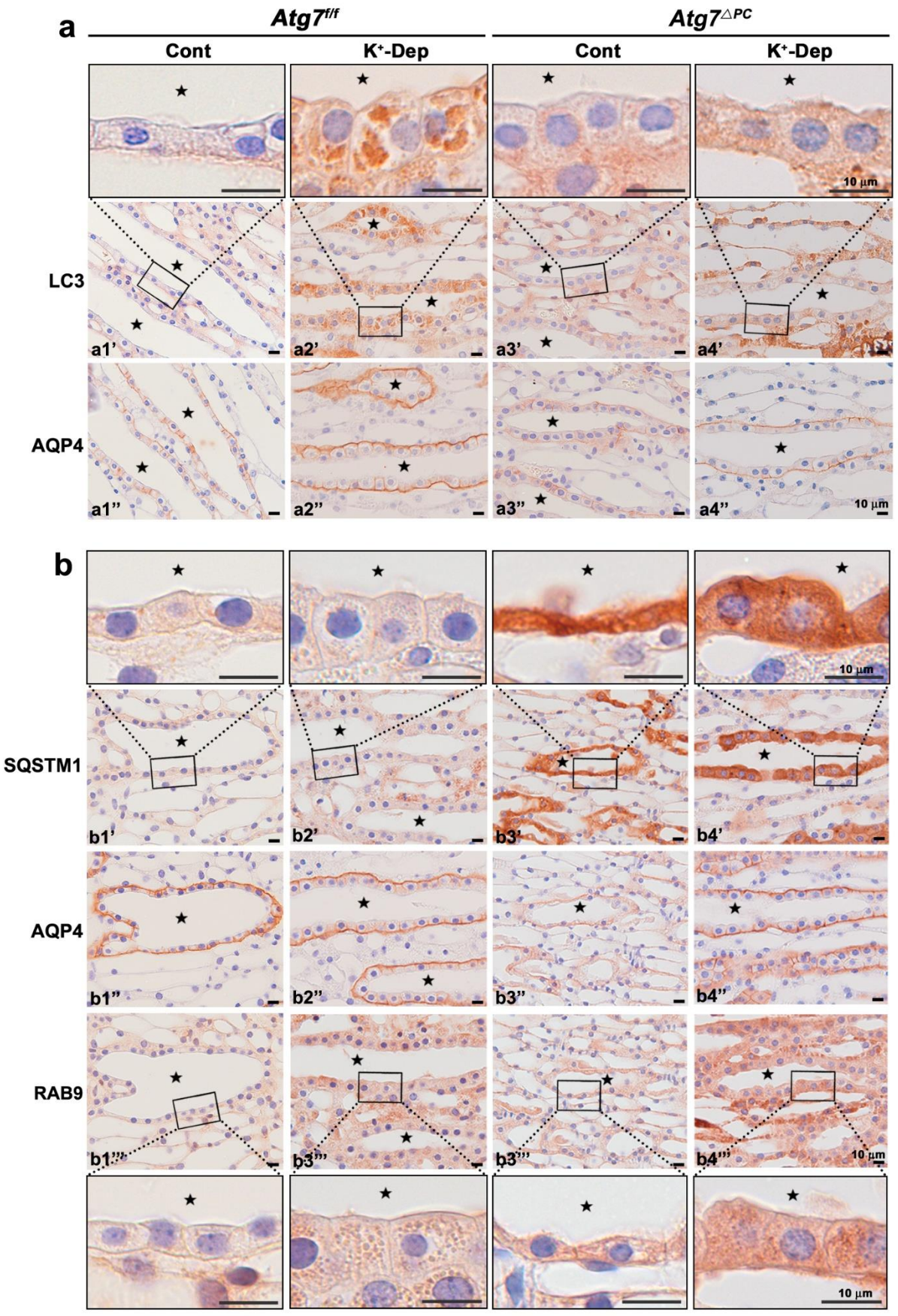
a
Atg7f/f
Atg7△PC
Cont
K+-Dep
Cont
K+-Dep
LC3
AQP4
a1'
a2'
a3'
a4'
a1"
a2"
a3"
a4"
10 μm
b
SQSTM1
AQP4
RAB9
b1'
b2'
b3'
b4'
b1"
b2"
b3"
b4"
b1'''
b3'''
b3'''
b4'''
10 μm

Figure S1. Light micrographs of the inner medulla of control (Cont) and K^+-depleted (K^+-Dep) *Atg7*$^{f/f}$ and *Atg7*$^{\triangle pc}$ mouse kidneys illustrating immunolabeling of LC3 (**a1'-a4')**, SQSTM1 (**b1'-b4')** and RAB9 (**b1'"-b4'"")**. Inner medullary collecting ducts (IMCDs) (stars) were identified by immunolabeling on the basolateral plasma membrane for AQP4 using consecutive sections (**a1"-a4")** and (**b1"-b4")**. (**a)** In the images, it can be observed that the intense immunoreactivity for LC3 in K^+-Dep *Atg7*$^{f/f}$ mice is markedly and restrictively decreased in the AQP4-positive IMCD cells in K^+-Dep *Atg7*$^{\triangle pc}$ mice. (**b)** Strong immunoreactivity for SQSTM1 is observed restrictively in the AQP4-positive IMCD cells of *Atg7*$^{\triangle pc}$ mice. Note the prominent increase of RAB9 in K^+-Dep *Atg7*$^{\triangle pc}$ mice. Boxes in (**a**, **b)** are higher magnification of the areas indicated by the rectangles in upper or lower panels.

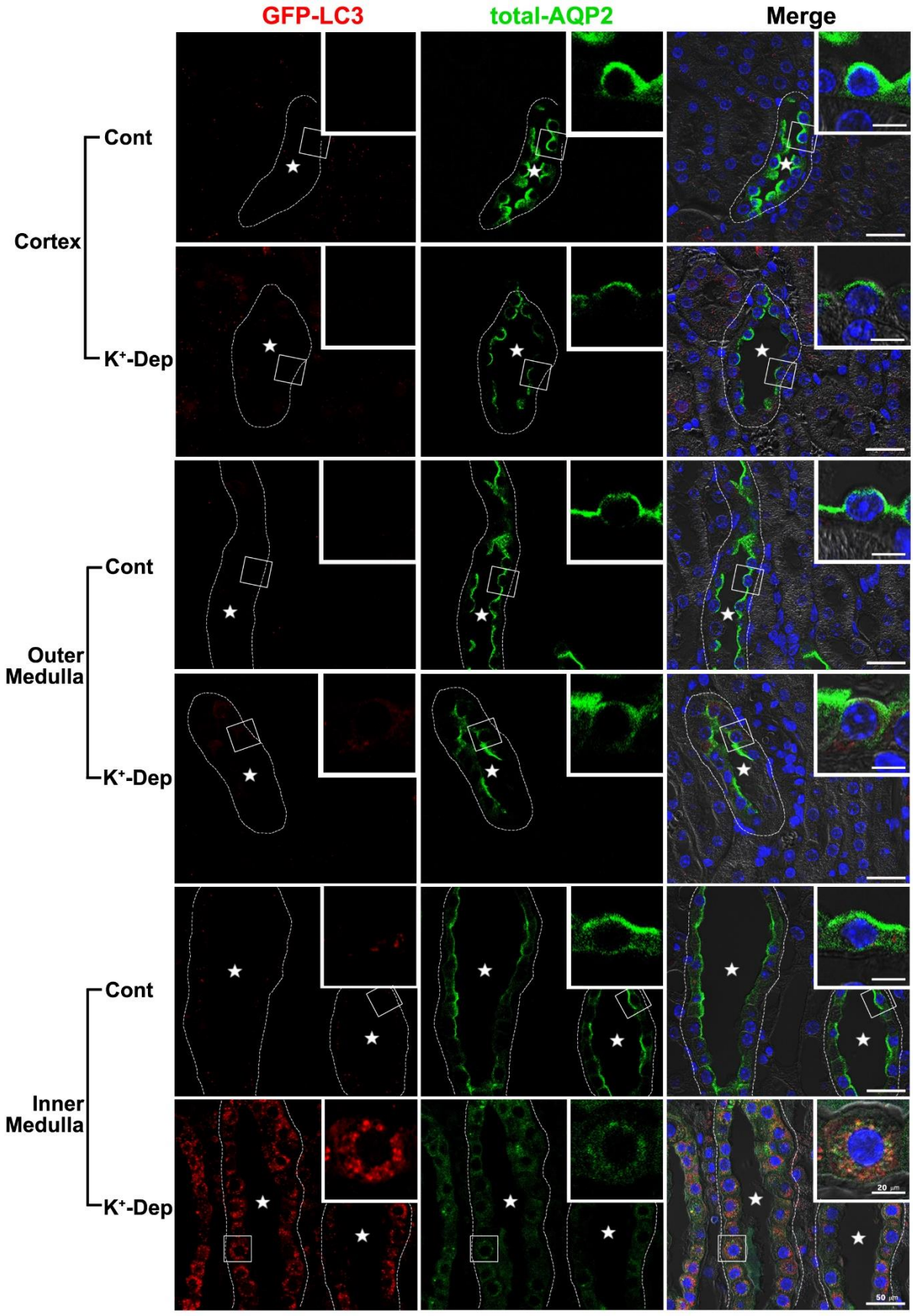

Figure S2. Confocal micrographs of the cortex, outer and inner medulla of control (Cont) and

K^+-depleted (K^+-Dep) GFP-LC3 transgenic mice illustrating double labeling with GFP-LC3 (red) and total-AQP2 (green). After potassium depletion for 2 weeks, GFP-LC3-positive dots are markedly accumulated in the inner medullary collecting duct (IMCD) cells, but a few in both cortical and outer medullary collecting duct cells. Note that total-AQP2 is colocalized with these GFP-LC3-positive puncta in the IMCD cells. Stars indicate the lumen of collecting ducts.

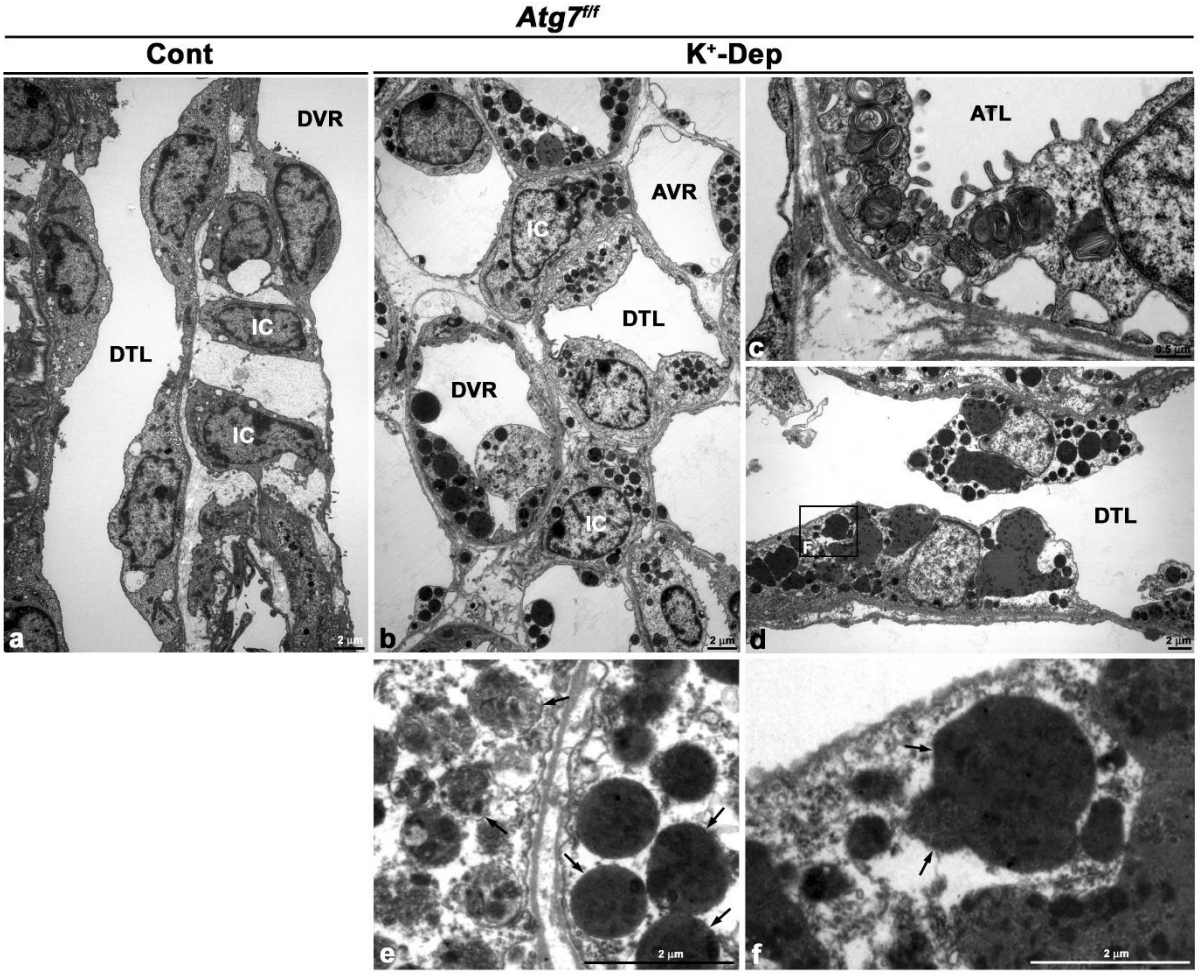

Figure S3. Transmission electron micrographs of the inner medulla of *Atg7*$^{f/f}$ mouse kidneys. (**a**). On normal diet (Cont), no autophagic vacuoles are observed in the cytoplasm of interstitial cell (IC), descending thin limb (DTL), or descending vasa recta (DVR). (**b**-**f)** After K^+-depletion (K^+-Dep), the accumulation of numerous autophagic vacuoles containing multilamellar bodies or degradation materials can be observed in the IC, DTL, ascending thin limb (ATL), DVR, and ascending vasa recta (AVR). (**f)** Higher magnifications of the areas outlined in (**d)**. A single membrane (arrows) can be observed surrounding various autophagic vacuoles.

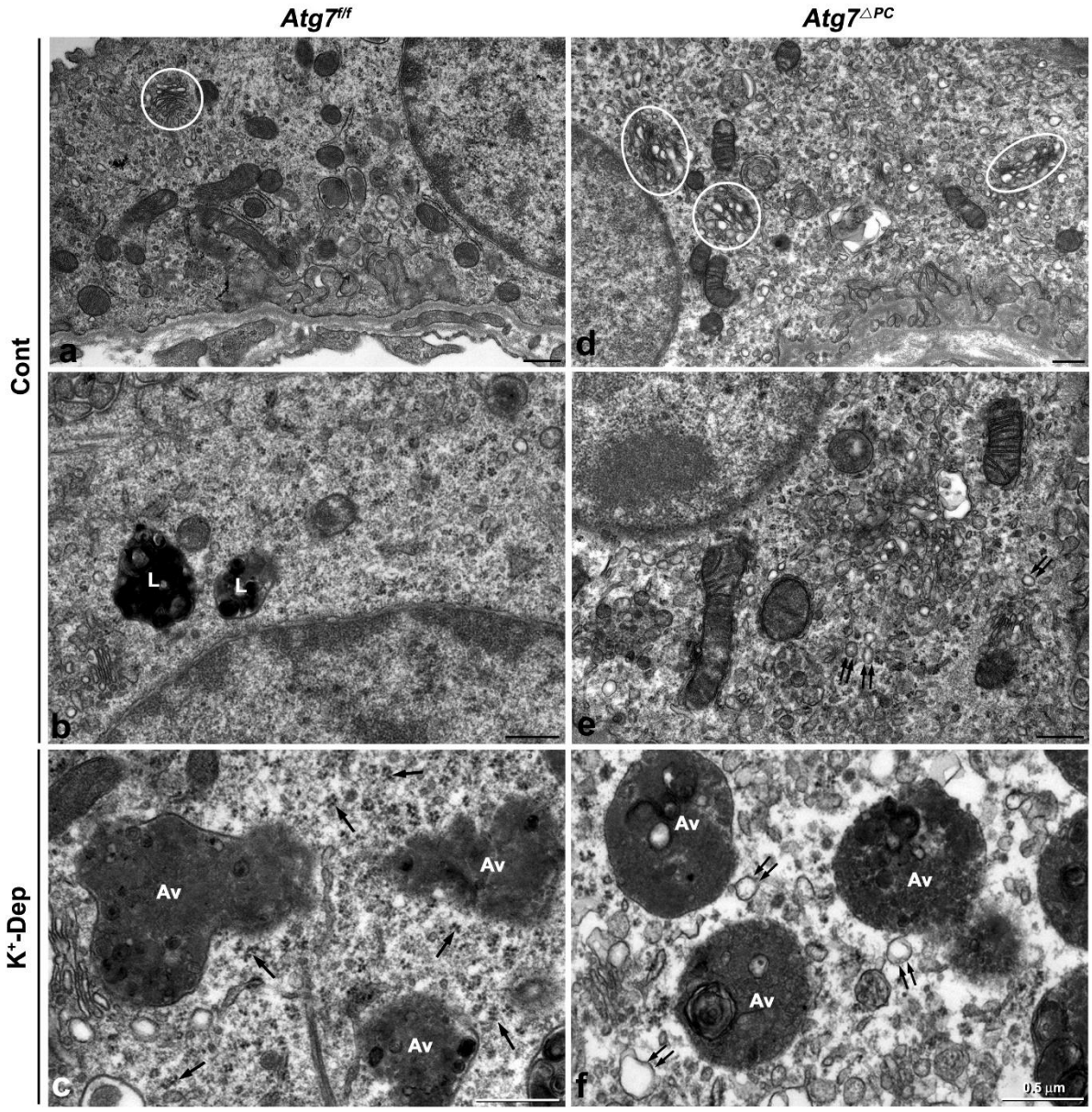

Figure S4. Transmission electron micrographs of inner medullary collecting duct (IMCD) cells. **(a-c)** In *Atg7*$^{f/f}$ mice, polysomes (arrows) are markedly increased throughout the cytoplasm in IMCD cells, as are autophagic vacuoles (Av) after K^+-depletion (K^+-Dep). **(d-f)** In *Atg7*$^{\triangle pc}$ mice, in contrast, Golgi complexes (circles) and small tubuloalveolar shaped vesicles (double arrows) are markedly increased in both control (Cont) and K^+-Dep groups.

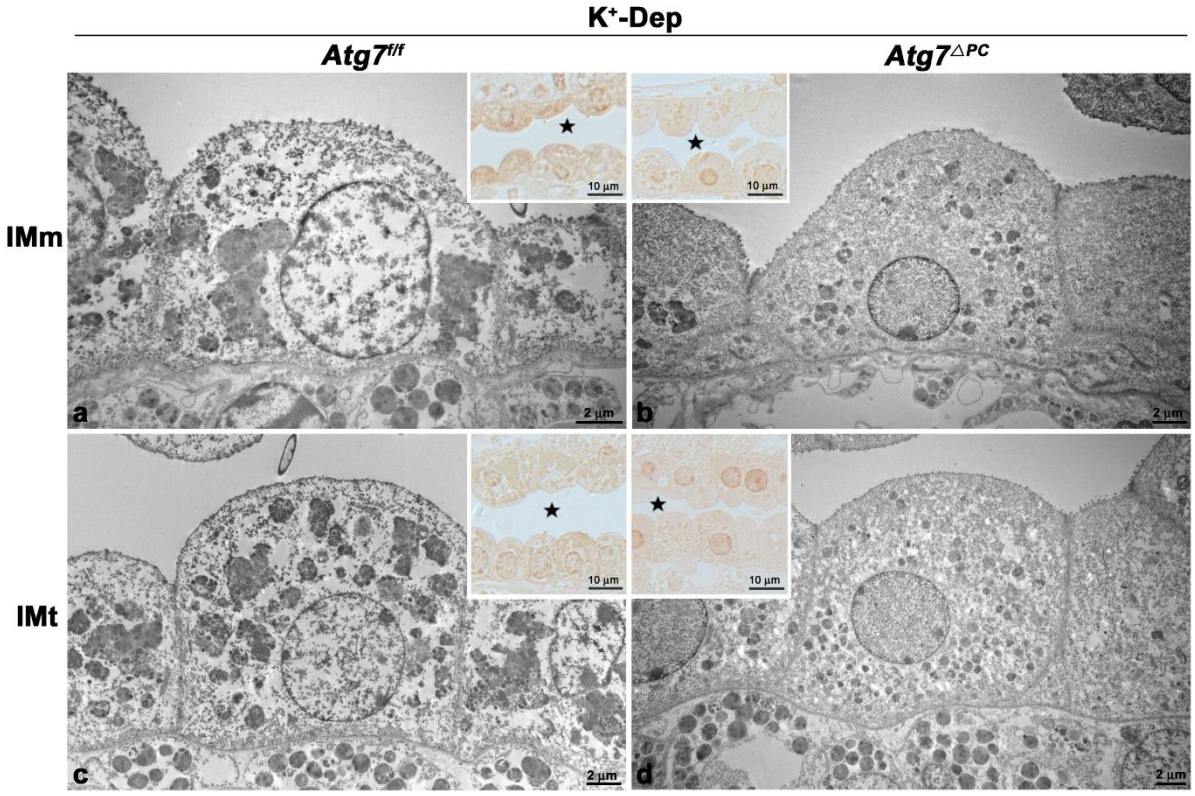

Figure S5. Immunoelectron micrographs of the middle (IMm). **(a**, **b)** and the terminal (IMt). **(c**, **d)** parts of the inner medulla of K^+ depleted (K^+-Dep) *Atg7*$^{f/f}$. **(a**, **c)** and *Atg7*$^{\triangle pc}$ **(b**, **d)** mice illustrating immunostaining for pS256-AQP2. The inserts are light micrographs of 1 m-thick semi-thin sections of the same group. No immunoreactivity of pS256-AQP2 is observed in either the canonical autophagic vacuoles in K^+-Dep *Atg7*$^{f/f}$ mice **a**, **c** or the non-canonical autophagic vacuoles in K^+-Dep *Atg7*$^{\triangle pc}$ mice **(b, d).** Stars indicate the lumen of inner medullary collecting ducts **(a-d)**.

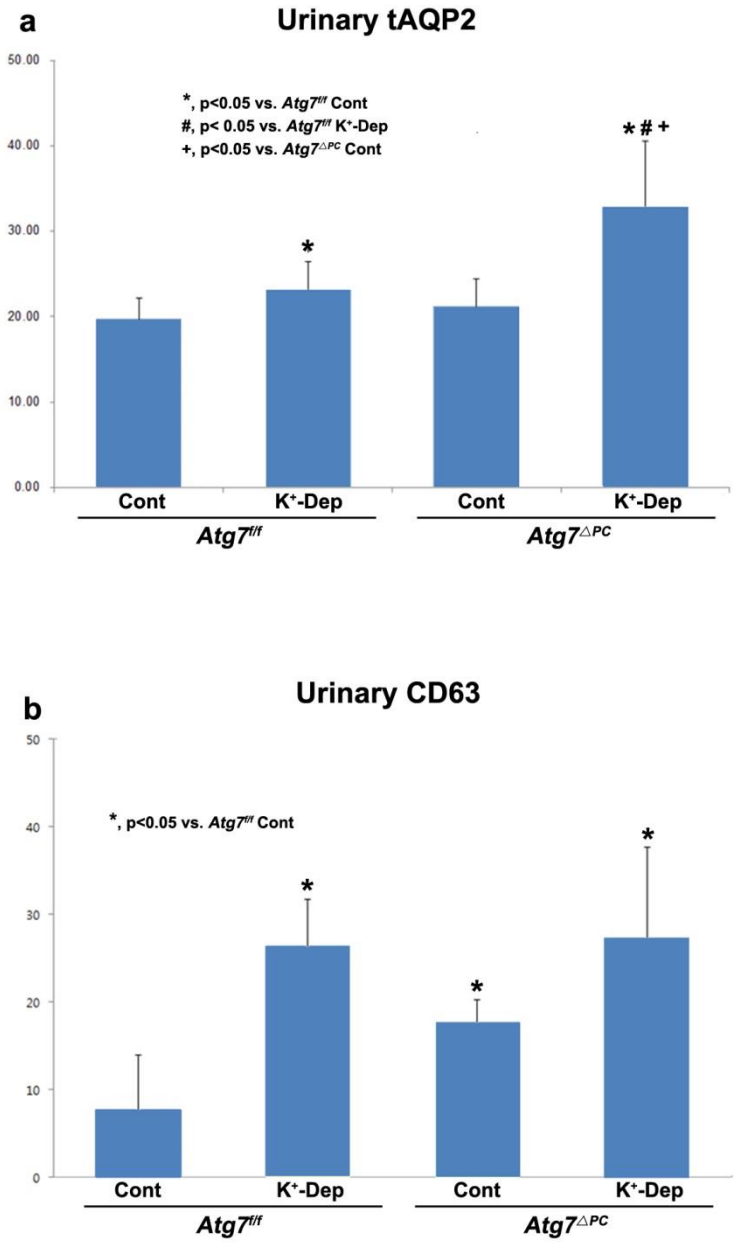

Figure S6. Enzyme-linked immunosorbent assay of urinary total-AQP2 (**a**) and CD63 (**b**). Note that urinary excretion of total-AQP2 and CD63 are significantly increased after K^+ depletion in both *Atg7*$^{f/f}$ mice and *Atg7*$^{\triangle pc}$ mice compare to those of control mice.